PHYSICAL REVIEW B **80**, 241405(R) (2009)

Excited states of biological chromophores studied using many-body perturbation theory: Effects of resonant-antiresonant coupling and dynamical screening

Yuchen Ma,[1,*] Michael Rohlfing,[1] and Carla Molteni[2]
[1]*Fachbereich Physik, Universität Osnabrück, D-49069 Osnabrück, Germany*
[2]*Physics Department, King's College London, Strand, London WC2R 2LS, United Kingdom*
(Received 2 November 2009; published 4 December 2009)

The excited states of model chromophores of the photoactive yellow protein and of rhodopsin are studied using *ab initio* many-body perturbation theory (within the GW approximation and Bethe-Salpeter equation). Calculations beyond the Tamm-Dancoff approximation, i.e., consideration of the resonant-antiresonant transition coupling, are needed for an accurate description of the lowest $\pi \rightarrow \pi^*$ excitations due to the large exchange interaction between the electron and hole localized in the low-dimension systems. The inclusion of dynamical effect in the electron-hole screening is important for an accurate description of the lowest $n \rightarrow \pi^*$ excitations.

DOI: 10.1103/PhysRevB.80.241405 PACS number(s): 87.15.M−, 71.15.Qe, 78.40.−q, 87.15.A−

The photoactive yellow protein (PYP) and rhodopsin are photoreceptors that transform light into biological signals. Their photocycles are initiated by the photoinduced isomerization of the small chromophores, *p*-coumaric acid (pCA) for PYP and the protonated Schiff base of retinal for rhodopsin. Because of their unique biochemistry and photophysical properties, these chromophores have been the subject of several spectroscopic investigations.[1–3] To explain the very first photoresponse of these chromophores, their excited states have been studied at various levels of quantum theory,[3–8] ranging from time-dependent density-functional theory (TDDFT) to coupled cluster methods and second-order perturbation-theory techniques like CASPT2. However, due to the complexity in the excited states, whose description must include not only the electron-electron (*e-e*) but also the electron-hole (*e-h*) interaction, the agreement between the as-obtained theoretical results and the experimental ones are not good. At variance from excitons in three-dimensional extended systems where the electron and hole are loosely bound, excitons (Coulomb-correlated *e-h* pair created by a photon) in chromophores are confined to a quasi-zero-dimensional space, where the *e-e* and *e-h* exchange and correlation interactions and the excitonic binding energy are large. This imposes the requirement on the high-order interactions within electrons and excitons as discussed below for a correct description of the excitations in the chromophores.

Many-body perturbation theory (MBPT) has been widely and successfully used for optical excitations in many systems, including crystals, clusters and molecules.[9–12] In this work, we test the importance of effects such as those of the resonant-antiresonant coupling (RARC) and of the dynamical screening, which are commonly neglected in the calculation of optical spectra, for biological chromophores, so to provide a set of guidelines for future studies of excitations in similar low-dimensional systems by MBPT and other theoretical methods.

Within MBPT, electronic exchange and correlation effects are included in the electron self-energy operator in terms of Hedin's *GW* approximation (GWA),[13] accompanied by the solution of the Bethe-Salpeter equation (BSE) for correlated *e-h* excitations from first principles.[9,14] Within the Tamm-Dancoff approximation (TDA) which is commonly employed for the calculation of optical spectra, only the resonant part of the BSE Hamiltonian is taken into account, while the coupling between transitions of the positive (resonant part) and negative (antiresonant part) frequencies are neglected.[14] However, TDA breaks down for the electron-energy-loss spectra of silicon[15] and the response properties of carbon nanotubes at high energy region where mixing of exciton and plasmon emerges.[16] TDA is also found to overestimate the absorption peak of *trans*-azobenzene by 0.2 eV.[16] In this Rapid Communication we show that the influence of RARC in the investigated biological chromophores can amount to $0.4 \sim 0.5$ eV for the lowest $\pi \rightarrow \pi^*$ excitation due to the large *e-h* exchange interaction; hence, it cannot be neglected.

Dynamical screening effects in the *e-h* interaction have been found to be crucial for core excitons.[17,18] For valence excitons, the dynamical effects (<0.1 eV for the excitation energy) can be neglected when the excitonic binding energies are much smaller than the plasma frequencies [or the quasiparticle (QP) band gap] of the investigated system.[9,14] Here we demonstrate that in biological chromophores the dynamical corrections for the $n \rightarrow \pi^*$ excitations are prominent and cannot be ignored, while those for the $\pi \rightarrow \pi^*$ excitations are significantly smaller.

MBPT calculations begin with conventional DFT calculations, followed by QP band-structure and optical excitation calculations within the *GW*+BSE approach. The frequency dependence of the screening and its influence on the self-energy operator in GWA and the *e-h* interaction in BSE are described by a generalized plasmon-pole model (PPM).[9,19]

For singlet-to-singlet excitations, the generalized BSE takes the form[14]

$$\begin{pmatrix} R & C \\ -C^* & -R^* \end{pmatrix} \begin{pmatrix} A \\ B \end{pmatrix} = \Omega \begin{pmatrix} A \\ B \end{pmatrix}, \tag{1}$$

with $R = D + 2K^{R,x} + K^{R,d}$, $C = 2K^{C,x} + K^{C,d}$, and $D \triangleq (E_c^{QP} - E_v^{QP})$.[9] R and $-R^*$ are the Hamiltonians corresponding to the resonant and the antiresonant parts of the transitions, respectively, while C and $-C^*$ are the coupling terms between the resonant ($v \rightarrow c$) and antiresonant ($c \rightarrow v$) transitions. $K^{R,x}(K^{R,d})$ and $K^{C,x}(K^{C,d})$ are the bare ex-

change term (screened direct term) of the *e-h* interaction kernel for the resonant transition and the corresponding coupling terms, respectively. E_c^{QP} and E_v^{QP} are the quasiparticle energies for the unoccupied (conduction) and occupied (valence) orbitals, respectively. Ω is the excitation energy. Within TDA, C is assumed to be zero; this is a good approximation for cases where the coupling terms are much smaller than the resonant and antiresonant terms. If C is comparable to R, one has to solve the eigenvalue problem in Eq. (1) with a non-Hermitian Hamiltonian. The eigenvalues of the non-Hermitian Hamiltonian can be found by Cholesky decomposition.[20]

Within PPM, the direct interaction of the resonant transition $K^{R,d}$ is calculated by[9]

$$K^{R,d}_{vc,v'c'}(\Omega) = -\sum_l \int d\mathbf{x}d\mathbf{x}'\,\psi_c^*(\mathbf{x})\psi_{c'}(\mathbf{x})\psi_v(\mathbf{x}')\psi_{v'}^*(\mathbf{x}') \times W_l(\mathbf{r},\mathbf{r}')\frac{z_l\omega_l}{2}\left[\frac{1}{\omega_l-(\Omega-(E^{QP}_{c'}-E^{QP}_{v'}))} + \frac{1}{\omega_l-(\Omega-(E^{QP}_{c}-E^{QP}_{v}))}\right], \quad (2)$$

where ω_l is the plasmon frequency and $W_l(\mathbf{r},\mathbf{r}')$ is the spatial behavior of the screened interaction at the plasmon mode l. z_l is a parameter to reproduce the static limit of the dielectric function. The matrix elements of $K^{C,d}$ have a similar form. The direct interaction is responsible for the binding between electron and hole in the exciton. The static screening [i.e., approximating both energy denominators in Eq. (2) to ω_l] constitutes the main part of the *e-h* attraction, while the dynamical effects are usually much smaller and can thus be considered as a perturbation to the results from static screening. The BSE including dynamical effects is solved through first-order perturbation theory, i.e., by

$$\delta\Omega = \sum_{vc,v'c'} A^*_{vc}[K^{R,d}_{vc,v'c'}(\Omega) - K^{R,d}_{vc,v'c'}(\text{static})]A_{v'c'}. \quad (3)$$

Note that the underlying *GW* single-particle levels are calculated from dynamical screening in all cases.

We select two PYP model chromophores, *p*-coumaric acid (*p*CA) and deprotonated thiomethyl *p*-coumaric acid (TmpCA^-), and one retinal chromophore, 11-*cis* protonated Schiff base of retinal (PSB11) as shown in Fig. 1. *p*CA is charge neutral, while the others are singly charged systems (TmpCA^- is negatively charged while PSB11 is positively charged). Reliable experimental data for the lowest excitation energies are available and provide a good benchmark for the theory.[1,3]

The ground-state geometries are optimized within DFT with the SIESTA code,[21] using Troullier-Martins pseudopotential and the Perdew-Burke-Ernzerhof exchange-correlation functional with double ζ plus a single shell of polarization function as basis set. The excitation energies are then calculated for the ground-state structures according to the Franck-Condon principle. Gaussian orbitals are used as basis functions to represent quantities occurring in the *GW* self-energy operator and the electron-hole interaction in BSE.

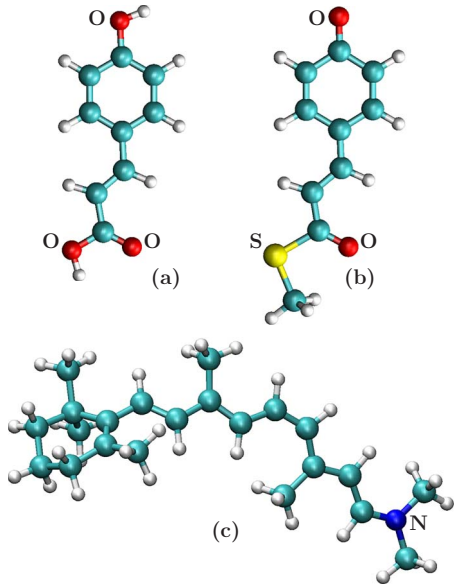

FIG. 1. (Color online) Structures of the PYP and retinal chromophores studied in this work: (a) *p*-coumaric acid, (b) deprotonated thiomethyl *p*-coumaric acid, and (c) 11-*cis* protonated Schiff base of retinal. O, S, and N represent oxygen, sulfur and nitrogen atoms, respectively, while the large circles and the small circles without element symbols represent carbon and hydrogen atoms, respectively.

Within TDA and the static limit of the $e-h$ direct interaction (see the third column of Table I), the calculated energies for the lowest excited state (S_1) are about 0.6 eV higher than the experimental values for the charged systems and 0.4 eV for the neutral *p*CA. For the two charged molecules, the

TABLE I. The lowest two excitation energies (in eV) of PYP and retinal chromophores calculated by different approaches and their comparison with reference experimental values. The third column ("TDA") refers to calculations within the Tamm-Dancoff approximation while the fourth and fifth columns ("full BSE") include resonant-antiresonant coupling [cf. Eq. (1)]. While the third and fourth columns have been obtained from static screening for the *e-h* interaction, dynamical effects are included in the fifth column by perturbation theory [cf. Eq. (3)].

		MBPT			
		TDA	Full BSE		
State		Sta.	Sta.	Dyn.	Exp.
*p*CA	S_1	4.46	4.06	3.94	4.06,[b] 4.00[d]
	S_2	4.25	4.33	4.20	4.37[b]
TmpCA^-	S_1	3.34	2.91	2.80	2.78[c]
	S_2	3.44	3.44	3.19	3.14[c]
PSB11	S_1	2.61	2.13	2.04	2.03[a]
	S_2	3.29	3.05	3.01	3.18[a]

[a]Reference 1.
[b]Reference 3.
[c]Reference 5.
[d]Reference 22.

TABLE II. Diagonal matrix elements $E_c^{QP}-E_v^{QP}$, $K_{vc,vc}^{R,d}$, $K_{vc,vc}^{C,d}$, $K_{vc,vc}^{R,x}(=K_{vc,vc}^{C,x})$, $R_{vc,vc}$, and $C_{vc,vc}$ for selected transitions $v\rightarrow c$ for TmpCA$^-$ and PSB11 (in eV). H and L denote HOMO and LUMO, respectively. The HOMO$\rightarrow$LUMO and HOMO$-1\rightarrow$LUMO transitions are the main components of the S_1 and S_2 excited states for TmpCA$^-$ and PSB11, respectively.

	v	c	$E_c^{QP}-E_v^{QP}$	$K^{R,d}$	$K^{C,d}$	$K^{R/C,x}$	R	C
TmpCA$^-$	$H-1$	L	7.81	−4.23	−0.08	0.10	3.78	0.12
	H	L	6.03	−4.53	−0.56	1.50	4.50	2.44
PSB11	$H-1$	L	5.62	−3.58	−0.34	0.97	3.98	1.60
	H	L	4.50	−3.58	−0.45	1.19	3.30	1.93

S_1 state is predominantly a $\pi\rightarrow\pi^*$ transition (80–90 % of the oscillator strength) from the highest occupied molecular orbital (HOMO) to the lowest unoccupied molecular orbital (LUMO). For the neutral *p*CA, however, the TDA places the HOMO$\rightarrow$LUMO (at 4.46 eV) above another transition (at 4.25 eV). Going beyond the TDA lowers the former by 0.4 eV and raises the latter by 0.08 eV, thus changing the ordering of the two states and yielding the HOMO$\rightarrow$LUMO$\pi\rightarrow\pi^*$ dominated transition (labeled S_1) as the onset of the spectrum.

Inclusion of RARC decreases the energies of the S_1 states for the three molecules by 0.4–0.5 eV. In molecules where the RARC effects are negligible, e.g., SiH_4, the diagonal matrix elements $K_{vc,vc}^{R,x}$, $K_{vc,vc}^{C,x}$, and $K_{vc,vc}^{C,d}$ are usually smaller than 5% of $K_{vc,vc}^{R,d}$; the matrix elements $C_{vc,vc}$ for the coupling term are also smaller than 5% of $R_{vc,vc}$ for the resonant part for the transitions $v\rightarrow c$. For the S_1 state in the three selected chromophores, the size of $C_{vc,vc}$ for the HOMO$\rightarrow$LUMO transition can be up to 60% of $R_{vc,vc}$ as shown in Table II. This is mainly due to the large exchange interaction between electron and hole. For higher $\pi\rightarrow\pi^*$ excitations, such as S_2 in PSB11, the RARC correction to the excitation energies is much weaker because of the smaller exchange interaction and the larger QP transition energy between the electron at LUMO and the hole at HOMO-1. The S_2 state in *p*CA is also of $\pi\rightarrow\pi^*$ type but is composed of more transitions (mainly HOMO$-2\rightarrow$LUMO+1, HOMO$\rightarrow$LUMO, and HOMO$\rightarrow$LUMO+1) in a complex way; here the inclusion of the coupling terms increases the excitation energy by a small amount at variance from the other $\pi\rightarrow\pi^*$ excitations where the excitation energies are lowered.

The S_2 states in TmpCA$^-$ is of $n\rightarrow\pi^*$ character, with the n orbital relating to the lone pair of the phenolic oxygen. The $n\rightarrow\pi^*$ excitation is dominated by the HOMO$-1\rightarrow$LUMO transitions. The exchange interaction between the HOMO-1 and LUMO and the RARC terms are very small as shown in Table II. Hence, TDA is accurate enough for the $n\rightarrow\pi^*$ excitation. Note that the oscillator strength of the $n\rightarrow\pi^*$ excitation is orders of magnitude smaller than that of the $\pi\rightarrow\pi^*$ excitation, so it contributes only weakly to the optical spectrum.

Since the RARC effect is stronger in PSB11 where the HOMO and LUMO are localized on the polyene chain,[8] we may conclude that the short polyene chain present in the chromophores is responsible for the strong RARC effect. By calculating the excitation energy of polyene chains (C_nH_{n+2}) with different length, we find that the RARC effect diminishes gradually for the lowest bright exciton, from 0.75 eV for $n=4$, 0.48 eV for $n=16$, to 0.12 eV for $n=32$, due to the wider spread of HOMO and LUMO with the increasing of chain length. We should mention here that although the RARC effect is small for the lowest bright excited state of $C_{32}H_{34}$, the RARC term still cannot be neglected since the order of its lowest two excited states, one bright and one dark, is swapped from TDA to full BSE, the lowest being dark within the former and being bright within the latter. For more delocalized π-bonded systems, such as poly(*para*-phenylene) and (carbon or boron-nitride based) nanotubes, the error caused by employing the TDA is much smaller, about 0.1 eV for the former and nearly zero for the latter.

TABLE III. The dynamical screening corrections (Eq. (3)) to the lowest $n\rightarrow\pi^*$ excitation (state S_2) of TmpCA$^-$ arising from the diagonal matrix element (second row) and one off-diagonal matrix element (third row). $K_{vc,v'c'}^{R,d}$, $\delta K_{vc,v'c'}^{R,d}$ $[=K_{vc,v'c'}^{R,d}(\Omega)-K_{vc,v'c'}^{R,d}(\text{static})]$ and $\delta\Omega$ are in eV. H and L denote HOMO and LUMO, respectively.

v	c	v'	c'	A_{vc}	$A_{v'c'}$	$K_{vc,v'c'}^{R,d}$	$\delta K_{vc,v'c'}^{R,d}$	$\delta\Omega$
$H-1$	L	$H-1$	L	0.95	0.95	−4.23	−0.05	−0.05
$H-1$	L	$H-1$	$L+5$	0.95	−0.27	0.80	0.21	−0.06

TDDFT, another widely used *ab initio* method for studying the excited states of organic molecules, has a Hamiltonian formulation of the same form as Eq. (1), with the only difference with respect to BSE being that the dynamical screening interaction W in Eq. (2) is replaced by an exchange-correlation kernel.[14,23] Compared to the full TDDFT,[24] the Tamm-Dancoff approximation to TDDFT was found to give a 0.4∼0.5 eV higher excitation energy for short polyene chains, while the results from TDDFT/TDA agreed much better with experiments than the full TDDFT.[24] A recent TDDFT calculation draws an opposite conclusion that the full TDDFT is more appropriate than TDDFT/TDA for PSB11.[8] TDDFT has limitations in accurately describing the excitation of polyene chains and chromophores[25] and its performance depends strongly on the exchange-correlation kernel used. The important role of the exchange interaction demonstrated by our work can provide guidelines for the selection of exchange-correlation kernel for future TDDFT calculations of chromophores and similar systems.

Inclusion of the dynamical screening decreases the excitation energy by about 0.3 eV for the $n\rightarrow\pi^*$ transitions, but by only 0.1 eV for the $\pi\rightarrow\pi^*$ transitions. The direct interaction in the RARC part is much smaller than that in the resonant part, and the dynamical screening effects mainly come from the resonant part. Hence, here we only discuss the dynamical effects in $K^{R,d}$. The dynamical screening correction $\delta K_{vc,v'c'}^{R,d}(\omega)$ cannot be ignored when either (i) the excitonic binding energies are of the same order of magnitude as the characteristic frequencies ω_l occurring in the dielectric screening [cf. Eq. (2)] (this is the case for both the $\pi\rightarrow\pi^*$ and the $n\rightarrow\pi^*$ excitations in TmpCA$^-$, although the binding energies of the former are usually ∼1 eV smaller than the

latter); or (ii) the excitations are composed from free $e-h$ transitions with very different energies $(E_c^{QP}-E_v^{QP})$. For S_2 of $TmpCA^-$, which is the lowest $n\rightarrow\pi^*$ excitation, the contribution from the off-diagonal element of $K^{R,d}_{vc,v'c'}$, where $v\rightarrow c$ and $v'\rightarrow c'$ belong to different transitions, is the main part of the dynamical screening correction and amounts to −0.2 eV, and the largest off-diagonal contribution comes from the dynamical screening correction to $K^{R,d}_{\mathrm{HOMO-1,LUMO;HOMO-1,LUMO+5}}$ as shown in Table III. The large contribution from the off-diagonal terms results from the large contribution of the transition $v\rightarrow c$ with $v=\mathrm{HOMO}-1$ and $c\neq\mathrm{LUMO}$ to the lowest $n\rightarrow\pi^*$ transition, the amplitude $|A_{vc}|$ of which reaches 0.27 (see Table III). The contribution from the diagonal terms, e.g., $\delta K^{R,d}_{\mathrm{HOMO-1,LUMO;HOMO-1,LUMO}}$ as shown in Table III, is only −0.05 eV.

In conclusion, the excited states of PYP and retinal chromophore models can be accurately described within MBPT, if the resonant-antiresonant coupling beyond the commonly employed TDA (in particular for the $\pi\rightarrow\pi^*$ excitations), as well as dynamical screening effects in the *e-h* interaction (in particular for the $n\rightarrow\pi^*$ excitations) are included. The resonant-antiresonant coupling effect is pronounced for the lowest bright excited state of a linear molecule encompassing a short polyene chain.

This work has been supported by the Deutsche Forschungsgemeinschaft (Bonn, Germany) by Grant No. Ro 1318/4-3.

*yuma@uos.de

[1] I. B. Nielsen, L. Lammich, and L. H. Andersen, Phys. Rev. Lett. **96**, 018304 (2006).
[2] I. B. Nielsen, S. Boyé-Péronne, M. O. A. El Ghazaly, M. Brøndsted Kristensen, S. B. Nielsen, and L. H. Andersen, Biophys. J. **89**, 2597 (2005).
[3] M. de Groot, E. V. Gromov, H. Köppel, and W. J. Buma, J. Phys. Chem. B **112**, 4427 (2008).
[4] A. Sergi, M. Grüning, M. Ferrario, and F. Buda, J. Phys. Chem. B **105**, 4386 (2001).
[5] V. Molina and M. Merchán, Proc. Natl. Acad. Sci. U.S.A. **98**, 4299 (2001), and references therein.
[6] E. V. Gromov, I. Burghardt, H. Köppel, and L. S. Cederbaum, J. Am. Chem. Soc. **129**, 6798 (2007).
[7] S. Sekharan, O. Weingart, and V. Buss, Biophys. J. **91**, L07 (2006).
[8] M. T. Sun, Y. Ding, G. L. Cui, and Y. J. Liu, J. Phys. Chem. A **111**, 2946 (2007).
[9] M. Rohlfing and S. G. Louie, Phys. Rev. B **62**, 4927 (2000).
[10] E. L. Shirley, Phys. Rev. Lett. **80**, 794 (1998).
[11] L. X. Benedict, E. L. Shirley, and R. B. Bohn, Phys. Rev. Lett. **80**, 4514 (1998).
[12] S. Albrecht, L. Reining, R. Del Sole, and G. Onida, Phys. Rev. Lett. **80**, 4510 (1998).
[13] L. Hedin and S. Lundqvist, in *Solid State Physics: Advances in Research and Application*, edited by F. Seitz, D. Turnbull, and H. Ehrenreich (Academic, New York, 1969), Vol. 23, p. 1.
[14] G. Onida, L. Reining, and A. Rubio, Rev. Mod. Phys. **74**, 601 (2002).
[15] V. Olevano and L. Reining, Phys. Rev. Lett. **86**, 5962 (2001).
[16] M. Grüning, A. Marini, and X. Gonze, Nano Lett. **9**, 2820 (2009).
[17] G. Strinati, Phys. Rev. Lett. **49**, 1519 (1982).
[18] A. L. Ankudinov, A. I. Nesvizhskii, and J. J. Rehr, Phys. Rev. B **67**, 115120 (2003).
[19] M. Rohlfing, P. Krüger, and J. Pollmann, Phys. Rev. B **52**, 1905 (1995).
[20] P. Papakonstantinou, EPL **78**, 12001 (2007).
[21] J. M. Soler, E. Artacho, J. D. Gale, A. García, J. Junquera, P. Ordejón, and D. Sánchez-Portal, J. Phys.: Condens. Matter **14**, 2745 (2002).
[22] M. Putschögl, P. Zirak, and A. Penzkofer, Chem. Phys. **343**, 107 (2008).
[23] E. Runge and E. K. U. Gross, Phys. Rev. Lett. **52**, 997 (1984).
[24] C. P. Hsu, S. Hirata, and M. Head-Gordon, J. Phys. Chem. A **105**, 451 (2001).
[25] E. M. González, L. Guidoni, and C. Molteni, Phys. Chem. Chem. Phys. **11**, 4556 (2009).